

⁶Li-⁶Li and ⁷Li-⁷Li elastic scattering from 2.0 to 5.5 MeV

E. Norbeck, P. T. Wu,* C. R. Chen, and R. R. Carlson

Department of Physics and Astronomy, The University of Iowa, Iowa City, Iowa 52242

(Received 13 September 1982)

Elastic scattering of ⁶Li from ⁶Li and ⁷Li from ⁷Li has been studied for beam energies from 2.0 to 5.5 MeV using very thin films of isotopically separated LiF as targets. A double-folding model optical potential provided a good fit for ⁷Li+⁷Li for the entire energy range, and for ⁶Li+⁶Li for energies low enough that the breakup ⁶Li→α+d could not occur. For higher energies, the real part of the ⁶Li+⁶Li potential falls off rapidly with energy so that by 5.5 MeV the potential well required to fit the data is only about 40% as deep as is predicted by the folding model.

NUCLEAR REACTIONS ⁶Li(⁶Li,⁶Li) and ⁷Li(⁷Li,⁷Li), E_{lab}=2.0–5.5 MeV; measured σ(θ,E), calculated double-folding model potentials.

I. INTRODUCTION

Double-folding model potentials provide a good description of elastic scattering of intermediate energy heavy ions such as ¹²C and ¹⁶O.¹ But for ⁶Li, ⁷Li, and ⁹Be the calculated potentials are overpredicted by a factor of 2.² Coupled channel calculations for ⁶Li scattering from various heavy nuclei in the 20 to 200 MeV energy range have shown that this factor of 2 can be explained as a consequence of the low threshold for the breakup mode ⁶Li→α+d.³ If this explanation is correct, the discrepancy should be even larger for Li+Li scattering where both beam and target are subject to breakup, and the discrepancy should disappear when the beam energy is sufficiently low that the breakup cannot occur. The threshold beam energies are E_{lab}=2.94 MeV for ⁶Li+⁶Li→⁶Li+α+d and E_{lab}=4.93 MeV for ⁷Li+⁷Li→⁷Li+α+t.

The previous studies of Li+Li elastic scattering in the energy range studied here have not been of sufficient precision to allow meaningful theoretical fits to the data.^{4,5} For ⁶Li+⁶Li, there have been some scattered measurements at higher energies,^{5,6} but even for the best of these the overall normalization for the angular distributions was uncertain.

One of the goals of this work was to make precise cross-section measurements and use them along with the double-folding model to generate Li–Li potentials for DWBA calculations. For ⁶Li+⁶Li→3α with E_{lab}=2.0 MeV, our folding-model potential allowed an excellent fit⁷ to the data, while other reasonable potentials, which also fit the scattering data, failed.⁸

It is interesting that the double-folding model works so well for low-energy lithium ions. The model was developed for heavier ions at higher energies where only the outer edge of the potential affects the scattering cross section.⁹ With low-energy lithium ions, the interior of the potential is more important than the surface.¹⁰

II. EXPERIMENT

The lithium beams were supplied by The University of Iowa HVEC Model CN 6 MV Van de Graaff accelerator. Either ⁶Li or ⁷Li could be selected from a multiple hot-

filament ion source. The scattered beam was detected by two 100 μm thick silicon surface-barrier detectors at the outer edge of a 43 cm diameter Ortec Model 600 scattering chamber. The angular resolution of the detectors was about 1°. The signals were passed through Ortec 142B preamps and conventional electronics to an on-line CDC 160A computer system for storage and analysis. No particle-identification system was needed for energies up to 5.5 MeV, the background of nuclear reaction products being sufficiently small that it could be subtracted off without appreciable error.

The targets were made by evaporating isotopically pure (99.32% for ⁶Li, 99.99% for ⁷Li) LiF onto the thinnest, manageable Formvar films. The LiF layer was generally 10 to 20 μg/cm² thick. Figure 1 shows a typical pulse height spectrum from the detector. The carbon and oxygen in the target were mostly from the Formvar. The other elements were incorporated during the evaporation process.

The Formvar films were made by placing a small drop of ¼% Formvar in ethylene dichloride onto a very clean surface of cold distilled water in a 10 cm diameter dish in a laminar-flow hood. The films were left on the surface of the water for a number of minutes to make sure that all of the solvent had evaporated. If they were removed from

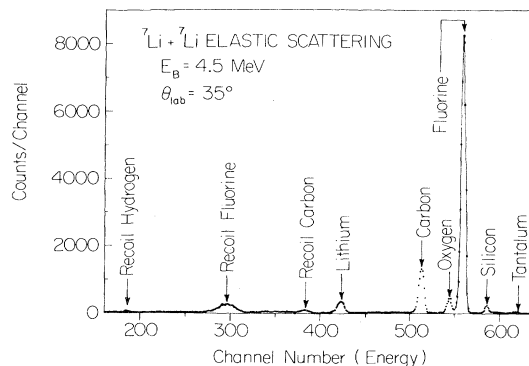


FIG. 1. Energy spectrum of ⁷Li beam scattered from a thin ⁷Li target.

the water too soon, they would shrink on the target frames and usually break when they were exposed to radiant heat during the LiF evaporation. The films were picked up onto thin, metal target frames that enclosed a 9 mm diameter hole. The film that extended beyond the edge of the target frame was cut away with a razor blade as it was being lifted from the water. The films were checked for uniformity and cleanliness by examination at both 100 and 400 times magnification with a Nomarski interference-contrast microscope.

When the Formvar film was adequately thin, it would usually break when LiF was evaporated onto it. This problem was overcome by first evaporating a small amount of LiF (10 mg) to stabilize the target backing. The film was then thick enough to withstand the evaporation of the rest of the LiF, typically about 50 mg. The evaporation of tantalum metal onto the target was prevented by keeping the temperature of the tantalum boat as low as possible. The distance between the tantalum boat and the mounted Formvar films was 20 cm. The vacuum was 10^{-8} Torr. A metal vane protected the film until the LiF began to melt, at which time the vane was moved aside with the aid of a magnet which was external to the vacuum system.

When LiF is evaporated from tantalum metal, a small part of the lithium is deposited as the metal. This should be expected; when Li_2CO_3 is evaporated from tantalum, most of the lithium comes off as the metal. The evidence for the deposition of lithium metal along with the LiF was the presence of basic compounds such as LiOH and Li_2CO_3 which were formed as soon as the metal came into contact with air. The basic compounds were detected in a film deposited on glass by using pH paper which turned from yellow to purple in the range 6.0 to 8.5. When the wet paper was rubbed over 0.5 cm^2 of surface, it turned purple. An area of glass that had been screened from the evaporating LiF served as a control. A test with the same kind of pH paper showed no trace of basic compounds in the LiF before it was evaporated. The Li-F atomic ratio has been used in many experiments, including this one, to determine absolute cross sections for lithium reactions. If some of the lithium atoms in the target are not accompanied by fluorine atoms, the ratio will not be unity. To minimize the deposition of metal, we tried to avoid heating the tantalum any hotter than necessary and to leave a little of the LiF behind in the boat.

To determine the Li-F atomic ratio in the target, we measured the area under the peaks in the energy spectrum corresponding to Li scattered from Li and F for a detector angle of 30° and a beam energy of 1.5 MeV. At this angle the resolution of the peaks was adequate, and at this energy the unknown nuclear force made no significant contribution to the scattering cross section. The measurements indicated that, with our method of evaporating the LiF, the excess of Li over F was never more than 5%. Appropriate corrections have been made to the data.

For each point in the angular distributions, the ratio of the cross section for Li+Li scattering to that for Mott scattering of identical particles in a $1/r$ potential was determined by comparing the areas under the Li and F peaks. By using the potentials of Poling *et al.*¹¹ in our op-

tical model program, we found that the deviation of the scattering from that predicted by the Rutherford formula for Li+F was negligible for beam energies up to 5.5 MeV. For a detector angle of 45° , the peaks in the energy spectrum were well resolved, but for small angles it was necessary to subtract the tails of the C and O peaks from the Formvar from the F peak. One detector was kept at a large angle to constantly monitor the C-O-F ratios. These ratios were transformed to the ratios appropriate for the smaller angles by using the angular distributions of Poling *et al.*¹¹ Small uncertainties in this process had a negligible effect on the ${}^7\text{Li}+{}^7\text{Li}$ cross sections because the amounts of C and O in the target were small compared with the amount of F.

All the measurements were repeated a number of times, each time with somewhat improved technique. The accuracy was estimated to be 1.5 to 2% for ${}^6\text{Li}$, and 2 to 3% for ${}^7\text{Li}$, although a few points might have been off by as much as 5%.

III. THE DOUBLE-FOLDING MODEL

A. Form of the double-folding optical potential

The double-folding model assumes that the nucleus-nucleus potential can be calculated in the obvious way from the nucleon-nucleon interaction and the nucleon densities of the incident and the target particles:

$$V(\vec{R}) = \int d^3\vec{r}_1 \int d^3\vec{r}_2 \rho(\vec{r}_1) \rho(\vec{r}_2) V(\vec{r}_{12}), \quad (1)$$

where \vec{R} is the distance between nuclei and \vec{r}_{12} is the distance between nucleons so that $\vec{r}_{12} = \vec{R} + \vec{r}_2 - \vec{r}_1$ as in Fig. 2. We have assumed that the functions in this expression can all be regarded as spherically symmetric. The nucleon-nucleon potential used here was developed by Satchler and Love,¹

$$V(r_{12}) = \sum_{i=1}^2 w_i \frac{\exp(-u_i r_{12})}{u_i r_{12}}, \quad (2)$$

where $w_1 = 6315$ MeV, $w_2 = -1961$ MeV, $u_1 = 4\text{ fm}^{-1}$, and $u_2 = 2.5\text{ fm}^{-1}$. They showed that the OPEP (one-pion exchange potential) term in the odd state force does not contribute to the direct term because of spin-isospin averaging if both Z and N are even for either the beam or the target. Fox¹² showed that the spin-isospin averaging also gives zero contribution by OPEP for ${}^6\text{Li}$. Thus Eq. (2) is a reasonable nucleon-nucleon interaction to use. For ${}^7\text{Li}$ we simply assumed that the extra contribution of the single, unpaired proton in ${}^7\text{Li}$ does not make a large con-

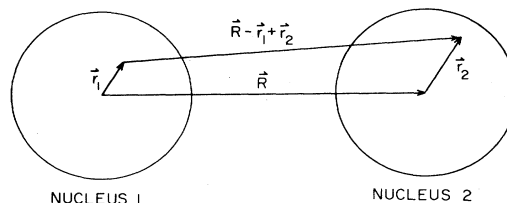


FIG. 2. Definition of coordinates used in Eq. (1).

tribution to the spin-isospin averaging for the ${}^7\text{Li} + {}^7\text{Li}$ potential.

Similarly, the double-folding Coulomb potential can be expressed by

$$V_c(\vec{R}) = \int d^3\vec{r}_1 \int d^3\vec{r}_2 \rho'(\vec{r}_1) \rho'(\vec{r}_2) V_c(\vec{r}_{12}), \quad (3)$$

where

$$\rho'(\vec{r}) = [Z\rho(\vec{r})/A]$$

is the charge density, and

$$V_c(\vec{r}_{12}) = (e^2/r_{12}).$$

The nuclear potential was taken to have the form $(V+iW)V(R)$, where the two parameters V and W were varied to optimize the fit. The folding model was considered correct if V turned out to be close to unity. The model did not predict W .

B. Formulation for ${}^7\text{Li} + {}^7\text{Li}$ elastic scattering

It is assumed here that the nucleon density is the same as that deduced from electron-scattering measurements. With a harmonic-oscillator model of the potential to bind the A nucleons together, the nucleon density is¹³

$$\rho(r) = \frac{2A\beta^3}{\pi^{3/2}(2+3\alpha)R_{\text{MS}}^3} \left[1 + \frac{\alpha\beta^2 r^2}{R_{\text{MS}}^2} \right] \exp \left[\frac{-\beta^2 r^2}{R_{\text{MS}}^2} \right], \quad (4)$$

where R_{MS} is the root-mean-square radius of the charge distribution, α is $(Z-2)/3 = \frac{1}{3}$, and

$$\beta^2 = \frac{3(2+5\alpha)}{2(2+3\alpha)}.$$

To make the correction for the finite size of the proton, we use the relation¹⁴

$$R_{\text{MS}}^2 = \langle r^2 \rangle - r_p^2, \quad (5)$$

where $\langle r^2 \rangle$ is the mean-squared radius of the charge distribution without correction, and r_p is the radius of the proton. Suelzle *et al.*¹⁴ obtained $\langle r^2 \rangle = (2.39 \text{ fm})^2$ from their electron scattering data. With $r_p = 0.836 \text{ fm}$,¹⁵ $R_{\text{MS}} = 2.239 \text{ fm}$.

To obtain the analytical expression for $V(R)$, we first use the relation

$$\frac{e^{-ur}}{r} = \frac{1}{2\pi^2} \int d^3\vec{k} \frac{e^{i\vec{k}\cdot\vec{r}}}{k^2 + u^2}. \quad (6)$$

Thus, Eq. (1) can be rewritten as

$$V(R) = \frac{1}{2\pi^2} \sum_{i=1}^2 \frac{w_i}{u_i} \int d^3\vec{k} \int d^3\vec{r}_1 \int d^3\vec{r}_2 \rho(\vec{r}_1) \rho(\vec{r}_2) \frac{e^{i\vec{k}\cdot\vec{R}} e^{i\vec{k}\cdot\vec{r}_2} e^{-i\vec{k}\cdot\vec{r}_1}}{k^2 + u_i^2}. \quad (7)$$

After carrying out the angular integrals, Eq. (7) becomes

$$V(R) = 32\pi \sum_{i=1}^2 \frac{w_i}{u_i} \int_0^\infty dk \frac{k^2 j_0(kR)}{k^2 + u_i^2} F_1(k) F_2(k), \quad (8)$$

where

$$F_i(k) = \int_0^\infty dr_i \rho(r_i) r_i^2 j_0(kr_i), \quad i=1,2 \quad (9)$$

are the form factors for the nucleon densities. Using the nucleon density in Eq. (4),

$$F_1(k) = F_2(k) = \frac{A}{4\pi} \left[1 - \frac{\alpha R_{\text{MS}}^2 k^2}{2\beta^2(2+3\alpha)} \right] \exp \left[\frac{-k^2 R_{\text{MS}}^2}{4\beta^2} \right]. \quad (10)$$

After putting this expression in Eq. (8), and carrying out a long but straightforward calculation, we get

$$V(R) = \frac{A^2}{2} e^{-R^2/4\gamma^2} \sum_{i=1}^2 \frac{w_i}{u_i} \left\{ (1 + u_i^2 d)^2 \frac{G_{u_i}^\gamma(R)}{R} - \pi^{-1/2} \left[\frac{2d}{\gamma^3} + d^2 \left(\frac{u_i^2}{\gamma^3} - \frac{3}{2\gamma^5} \right) + \frac{d^2 R^2}{4\gamma^7} \right] \right\}, \quad (11)$$

where

$$\gamma^2 = \frac{(2+3\alpha)R_{\text{MS}}^2}{3(2+5\alpha)}, \quad d = \frac{\alpha R_{\text{MS}}^2}{3(2+5\alpha)},$$

and

$$G_u^\gamma(R) = \exp \left[\gamma u - \frac{R}{2\gamma} \right]^2 \text{erfc} \left[\gamma u - \frac{R}{2\gamma} \right] - \exp \left[\gamma u + \frac{R}{2\gamma} \right]^2 \text{erfc} \left[\gamma u + \frac{R}{2\gamma} \right], \quad (12)$$

where erfc is the complimentary error function

$$\text{erfc}(x) = \frac{2}{\pi^{1/2}} \int_x^\infty e^{-t^2} dt = 1 - \text{erf}(x). \quad (13)$$

With the numerical values given above, $V(R) = -108$ MeV at $R = 0$.

For the double-folding Coulomb potential, we write

$$V_c(r_{12}) = e^2 \lim_{u \rightarrow 0} \frac{e^{-ur_{12}}}{r_{12}} \quad (14)$$

and follow the same steps as for the nuclear potential,

$$V_c(r) = 32\pi Z_1 Z_2 e^2 \lim_{u \rightarrow 0} \int_0^\infty dk \frac{k^2 j_0(kR)}{k^2 + u^2} \frac{F_1(k)}{A_1} \frac{F_2(k)}{A_2}, \quad (15)$$

where $F(k)$ is the same expression as in Eq. (10). Thus,

$$V_c(R) = Z^2 e^2 \left[\frac{\text{erf}(R/2\gamma)}{R} - \pi^{-1/2} \exp\left(\frac{-R^2}{4\gamma^2}\right) \left[\frac{d}{\gamma^3} - \frac{3d^2}{4\gamma^5} + \frac{d^2 R^2}{8\gamma^7} \right] \right]. \quad (16)$$

C. Formulation for ${}^6\text{Li} + {}^6\text{Li}$ elastic scattering

The nucleon density distributions in ${}^6\text{Li}$ and ${}^7\text{Li}$ are sufficiently different that the same formula cannot be used for both. For the ${}^6\text{Li}$ nucleus, we used the expression that Suelzle, Yearian, and Crannell¹⁴ found to give good fits to electron elastic-scattering measurements. They had analyzed their data with a multipole expansion and obtained the charge density

$$\rho(r) = \frac{A}{8\pi^{3/2}} \left[\frac{e^{-r^2/4a^2}}{a^3} + \frac{c^2}{b^5} \left[\frac{r^2}{4b^2} - \frac{3}{2} \right] e^{-r^2/4b^2} \right], \quad (17)$$

where a^2 , b^2 , and c^2 are parameters.

Using the same method as for ${}^7\text{Li}$, the form factors become

$$F_1(k) = F_2(k) = \frac{A}{4\pi} (e^{-k^2 a^2} - k^2 c^2 e^{-k^2 b^2}). \quad (18)$$

Following the method used by Payne and Nigam,¹⁶ we multiply F_1 and F_2 by $\exp(r_p^2 k^2/6)$ to correct for the finite size of the proton. The modified Suelzle medium radius parameters

$$a^2 = 0.87 \text{ fm}^2 - \frac{r_p^2}{6} = 0.7535 \text{ fm}^2,$$

$$b^2 = 1.7 \text{ fm}^2 - \frac{r_p^2}{6} = 1.5835 \text{ fm}^2,$$

and $c^2 = 0.205 \text{ fm}^2$, which give the best fit to the electron scattering data, also give the best fit to our data. With these parameters, the rms radius of the proton distribution is 2.398 fm. With Suelzle's other two parameter sets, the radii become 2.315 and 2.514 fm. These radii gave poorer fits to our data. The neutron distribution was assumed to be the same as the proton distribution. Putting Eq. (18) into Eq. (8), we get the nuclear potential

$$V(R) = \frac{A^2}{2R} \sum_i \frac{w_i}{u_i} \left\{ \exp\left(\frac{-R^2}{4\gamma_1^2}\right) G_{u_i}^{\gamma_1}(R) + 2c^2 \exp\left(\frac{-R^2}{4\gamma_2^2}\right) \left[u_i^2 G_{u_i}^{\gamma_2}(R) - \frac{R}{\pi^{1/2} \gamma_2^3} \right] + c^4 \exp\left(\frac{-R^2}{4\gamma_3^2}\right) \right. \\ \left. \times \left[u_i^4 G_{u_i}^{\gamma_3}(R) - \frac{R}{\pi^{1/2} \gamma_3^3} \left[u_i^2 - \frac{3}{2\gamma_3^2} + \frac{R^2}{4\gamma_3^4} \right] \right] \right\}, \quad (19)$$

where $\gamma_1^2 = 2a^2$, $\gamma_2^2 = a^2 + b^2$, and $\gamma_3^2 = 2b^2$. With the numerical values given above, $V(R) = -79$ MeV at $R = 0$.

By using expression (18) in Eq. (15), we obtain the Coulomb potential for ${}^6\text{Li} + {}^6\text{Li}$ elastic scattering,

$$V_c(R) = Z^2 e^2 \left[\frac{\text{erf}\left(\frac{R}{2\gamma_1}\right)}{R} - \frac{c^2}{\pi^{1/2} \gamma_2^3} \exp\left(\frac{-R^2}{4\gamma_2^2}\right) + \frac{c^4}{2\pi^{1/2} \gamma_3^5} \left[\frac{3}{2} - \frac{R^2}{4\gamma_3^2} \right] \exp\left(\frac{-R^2}{4\gamma_3^2}\right) \right]. \quad (20)$$

D. Extension of the model to ${}^7\text{Li} + {}^6\text{Li}$ elastic scattering

The elastic scattering ${}^7\text{Li} + {}^6\text{Li}$ is of particular interest because of the possibility of a resonant transfer of a neutron from ${}^7\text{Li}$ to ${}^6\text{Li}$.¹⁷ The products of the neutron transfer reaction would interfere coherently with the elastically scattered nuclei. The transfer reaction would be expected to show up as a deviation of the data from the predictions of the folding model, particularly at backward angles. For the folding model the nuclear potential is

$$V(R) = \frac{A_1 A_2}{2R} \sum_{i=1}^2 \frac{w_i}{u_i} \left\{ \exp \left[\frac{-R^2}{4\sigma_1^2} \right] \left[G_{u_i}^{\sigma_1}(R) + \xi u_i^2 G_{u_i}^{\sigma_1}(R) - \frac{\xi R}{\pi^{1/2} \sigma_1^3} \right] \right. \\ \left. + c^2 \exp \left[\frac{-R^2}{4\sigma_2^2} \right] \left[u_i^2 G_{u_i}^{\sigma_2}(R) - \frac{R}{\pi^{1/2} \sigma_2^3} + \xi u_i^4 G_{u_i}^{\sigma_2}(R) - \frac{\xi R}{\pi^{1/2} \sigma_2^3} \left(u_i^2 - \frac{3}{2\sigma_2^2} + \frac{R^2}{4\sigma_2^4} \right) \right] \right\}, \quad (21)$$

where

$$\sigma_1^2 = \frac{R_{MS}^2}{4\beta^2} + a^2, \quad \sigma_2^2 = \frac{R_{MS}^2}{4\beta^2} + b^2,$$

and

$$\xi = \frac{\alpha R_{MS}^2}{2\beta^2(2+3\alpha)}.$$

Similarly the Coulomb potential is

$$V_c(R) = Z_1 Z_2 e^2 \left[\frac{1}{R} \operatorname{erf} \left[\frac{R}{2\sigma_1} \right] - \frac{\xi}{2\pi^{1/2} \sigma_1^3} \exp \left[\frac{-R^2}{4\sigma_1^2} \right] + \frac{c^2}{2\pi^{1/2} \sigma_2^3} \exp \left[\frac{-R^2}{4\sigma_2^2} \right] \left(\frac{3\xi}{2\sigma_2^2} - \frac{\xi R^2}{4\sigma_2^4} - 1 \right) \right]. \quad (22)$$

IV. RESULTS

A. ${}^7\text{Li} + {}^7\text{Li}$ elastic scattering

The data and the folding-model fits to the data are shown in Figs. 3 and 4. For fits optimized at each energy, the normalization of the real potential varied randomly

between 1.011 and 1.095, presumably because of random errors in the data. The fits shown here were calculated using the values $V=1.030$ and $W=0.097$ for all energies. When this value of V was changed by 2%, the overall fit to the data was noticeably poorer. The difference between the optimal fit for a single beam energy and the overall fit is shown in Fig. 4 for 5.0 MeV where the difference is the

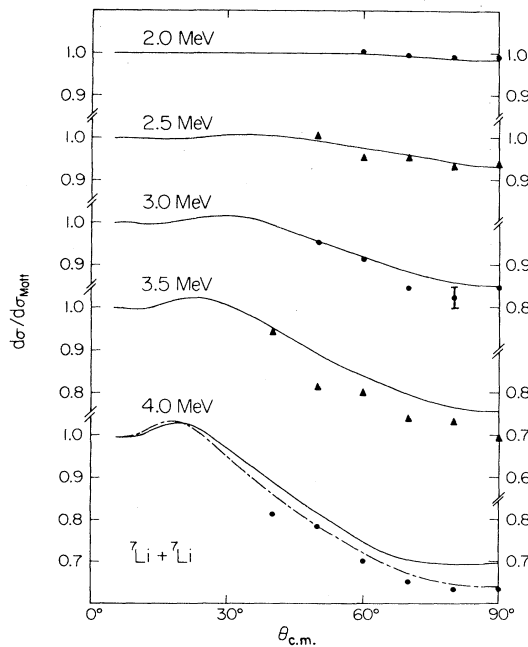


FIG. 3. ${}^7\text{Li} + {}^7\text{Li}$ elastic scattering data for beam energies from 2.0 to 4.0 MeV. The solid curves are the double-folding model fits with the proton finite size correction included, $V=1.03$ and $W=0.097$. The dotted-dashed curve at 4.0 MeV is the optimal fit without the correction, $V=1.0839$ and $W=0.1355$.

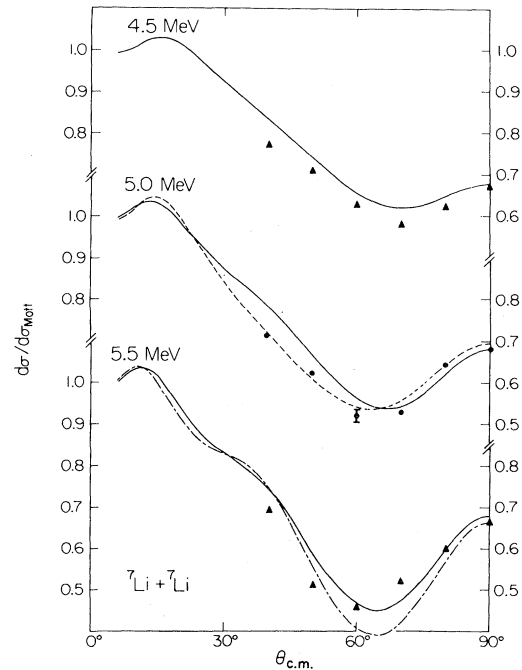


FIG. 4. Same as Fig. 3 except for beam energies from 4.5 to 5.5 MeV. The dashed curve at 5.0 MeV is the optimal fit with the proton finite size correction, $V=1.0896$ and $W=0.1035$. The dotted-dashed curve at 5.5 MeV is the optimal fit without the correction, $V=1.07$ and $W=0.881$.

largest. For 3.5, 4.0, and 4.5 MeV, the fits are worse than those for the other beam energies. If we do not take the finite size of the proton into account, we obtain slightly better fits for these three energies. An example is given for 4.0 MeV in Fig. 3. However, without the correction, we can never get a satisfactory fit to the 5.0 and 5.5 MeV data even if V and W are allowed to vary. An example is given for 5.5 MeV in Fig. 4. The correction for the finite size of the proton definitely improves the overall fit to the data. The poorer fits for 3.5 and 4.5 MeV could be due to resonance behavior, but are more likely due to small inaccuracies in the data.

Another overall fit to the data was obtained with $V=0.69$ and $W=0.075$. The curves provide a slightly better fit at 5.0 and 5.5 MeV and slightly worse at other energies. However, the curves for $V=0.69$ are not significantly different from those for $V=1.03$. For values of V midway between 1.03 and 0.69, no value of W would allow a good fit to the data.

Although 1.03 is closer to unity than 0.69, this fact by itself is not sufficient justification for rejecting the smaller value. An additional experimental test is provided by the total reaction cross section that can be predicted from the potential. These cross sections are shown in Table II. The available data are not good enough to allow a clear distinction between the two potentials, although from preliminary work done here,¹⁸ we would prefer the larger cross sections of the $V=1.03$ potential.

The almost equal quality fits with $V=0.69$ and 1.03 are

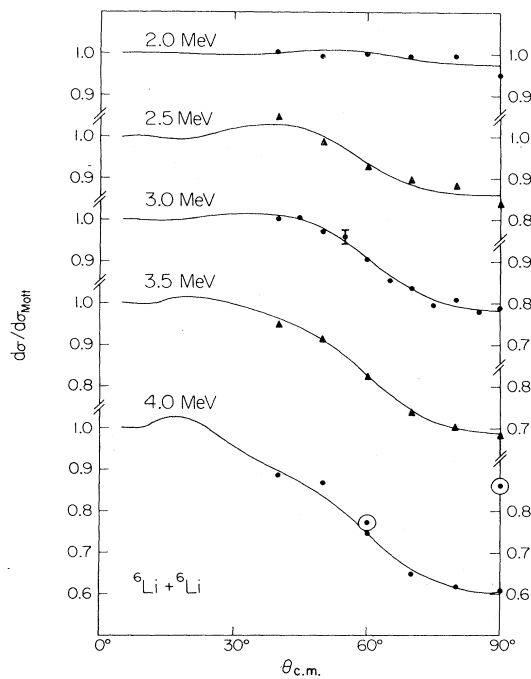


FIG. 5. ${}^6\text{Li}+{}^6\text{Li}$ elastic scattering data and the double-folding model fits for beam energies from 2.0 to 4.0 MeV. The proton finite size correction is included. The data points surrounded by circles are taken from Gruber *et al.* (Ref. 5). Values of V and W are given in Table I.

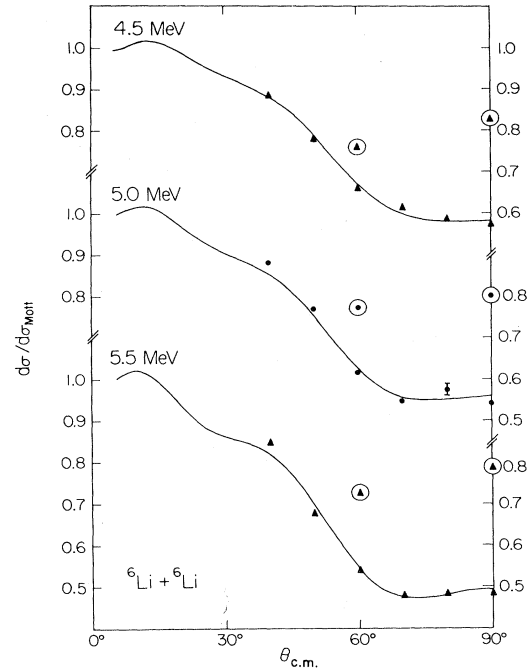


FIG. 6. Same as Fig. 5 except for beam energies from 4.5 to 5.5 MeV.

examples of the discrete ambiguity¹¹ where many discrete values of V can fit the experimental data equally well. Indeed, we could still fit the data with even larger V 's, but the total reaction cross sections predicted from the deeper potentials become unreasonably large.

B. ${}^6\text{Li}+{}^6\text{Li}$ elastic scattering

The data and the double-folding model fits are shown in Figs. 5 and 6. The values of V and W corresponding to the curves are listed in Table I. It can be seen that the folding model works well ($V=1$) for beam energies up to 3.0 MeV, which is the threshold energy (2.94 MeV) for the breakup process ${}^6\text{Li}\rightarrow\alpha+d$. As the beam energy increases, W rises rapidly and V falls. The total cross sections obtained are listed in Table II.

We tried nucleon-nucleon potentials other than the form in Eq. (2). Reference 1 gives several more complicated forms, but these all resulted in potentials that were either

TABLE I. Parameters of the double-folding optical model for the ${}^6\text{Li}({}^6\text{Li},{}^6\text{Li})$ reactions.

E_b (MeV)	V	W
2.0	0.9891	0.0876
2.5	1.0468	0.0564
3.0	0.9352	0.1502
3.5	0.8421	0.1875
4.0	0.7792	0.1473
4.5	0.5424	0.5221
5.0	0.4018	0.5379
5.5	0.4378	0.5160

TABLE II. Total reaction cross sections.

E_b (MeV)	${}^7\text{Li}+{}^7\text{Li}$		${}^6\text{Li}+{}^6\text{Li}$
	$V=1.03, W=0.097$ σ (mb)	$V=0.69, W=0.075$ σ (mb)	σ (mb)
2.0	27	21	40
2.5	94	74	130
3.0	209	170	251
3.5	346	293	381
4.0	470	409	488
4.5	563	499	558
5.0	637	565	602
5.5	704	622	681

too deep or too shallow to allow a good description of low energy ${}^6\text{Li}+{}^6\text{Li}$ elastic scattering.

The discrete ambiguity that was found for the ${}^7\text{Li}+{}^7\text{Li}$ fits exists also for the ${}^6\text{Li}+{}^6\text{Li}$ fits in the 2.0 to 3.0 MeV range. However, for higher beam energies, this effect no longer occurs. The values of V listed in Table I for beam energies higher than 3.0 MeV are the maximum values that can give good fits to the data. Of the many sets of V values that fit the data for beam energies less than 3.0 MeV, the set given in Table I is the only one that connects smoothly to that for higher energies.

The fact that this procedure yields a value of V close to unity for beam energies up to the breakup energy is an indication that the folding model is indeed giving an adequate potential. Since the model works for the ${}^6\text{Li}+{}^6\text{Li}$ case for beam energies below the breakup energy, it seems reasonable that a value of V close to unity is also the correct one for ${}^7\text{Li}+{}^7\text{Li}$ scattering below the ${}^7\text{Li}$ breakup energy (4.9 MeV).

We had hoped to fit the higher energy data published by other laboratories. Gruber *et al.*⁵ showed measurements for every 0.5 MeV from 4 to 20 MeV at 60° and 90° with complete angular distributions at 8.0, 10.0, 12.0, and 14.5 MeV. Fortune *et al.*⁶ gave complete angular distributions at 12, 20, and 28 MeV. The two publications are not in complete agreement. At 12 MeV both give the same cross section at 60° but differ by a factor of 2 at 90°. The overall normalization of the high energy data is in doubt. We wanted to make the data by Gruber *et al.*⁵ match ours from 4.0 to 5.5 MeV by multiplying all of Gruber's data by a single renormalization factor, but as can be seen easily from Figs. 5 and 6, no such factor can be chosen which will bring the two data sets into agreement.

V. DISCUSSION AND CONCLUSIONS

The double-folding model predicts the real part of the nuclear potential to within 10% for both ${}^6\text{Li}+{}^6\text{Li}$ and ${}^7\text{Li}+{}^7\text{Li}$ scattering if we use the simplest, realistic nucleon-nucleon interaction and if the beam energy is below the threshold for breakup.

Small differences in the effective nucleon-nucleon interaction can make large differences in the predicted scattering cross sections. Reference 1 offers improved versions of the interaction that take into account exchange effects and a density dependence. These give potentials that are the same in the peripheral region but are quite different in the interior. For heavy ions at intermediate energies, these various potentials are interchangeable, but in our case, where the inner part of the potential is the most important, only the original potential is compatible with the observed scattering cross sections. There are many corrections that must be made to the nucleon-nucleon interaction to adapt it to the high-density interior region. This work suggests that these corrections mostly cancel out.

We have shown that the magnitude of the ${}^6\text{Li}+{}^6\text{Li}$ potential predicted by the folding model must be reduced for energies above the breakup threshold. It would clearly be valuable to extend the ${}^7\text{Li}+{}^7\text{Li}$ measurements to higher energy to see if the ${}^7\text{Li}+{}^7\text{Li}$ potential behaves in the same way as the ${}^6\text{Li}+{}^6\text{Li}$ potential.

ACKNOWLEDGMENTS

We wish to thank C. P. Brown for his suggestions on methods for making thin targets. This work was supported in part by the U. S. Department of Energy.

*Present address: Institute of Nuclear Energy Research, Lung-Tan, Taiwan 325, The Republic of China.

¹G. R. Satchler and W. G. Love, Phys. Rep. **55**, 183 (1979).

²Z. Majka, H. J. Gils, and H. Rebel, Phys. Rev. C **25**, 2996 (1982).

³Y. Sakuragi, M. Yahiro, and M. Kamimura, Prog. Theor. Phys. **68**, 322 (1982); I. J. Thompson and M. A. Nagarajan, Phys. Lett. **106B**, 163 (1981); M. Kamimura, private communication.

⁴L. L. Pinsonneault and J. M. Blair, Phys. Rev. **141**, 961 (1966).

⁵G. Gruber, I. C. Dormehl, K. Meier-Ewert, and K. Bethge, Z. Phys. **265**, 411 (1973).

⁶H. T. Fortune, G. C. Morrison, and R. H. Siemssen, Phys. Rev. C **3**, 2133 (1971).

⁷E. Norbeck, C. R. Chen, M. D. Strathman, and D. A. Fox, Phys. Rev. C **23**, 2557 (1981).

⁸E. Norbeck, in *Scientific and Industrial Applications of Small Accelerators*, Proceedings of the Fourth Conference, 1976,

- edited by J. L. Duggan and I. L. Morgan (IEEE Service Center, Piscataway, N. J., 1976), p. 388.
- ⁹G. R. Satchler and W. G. Love, Phys. Lett. 65B, 415 (1976).
- ¹⁰E. Norbeck, M. D. Strathman, and D. A. Fox, Phys. Rev. C 18, 1275 (1978).
- ¹¹J. E. Poling, E. Norbeck, and R. R. Carlson, Phys. Rev. C 13, 648 (1976).
- ¹²D. A. Fox, M. S. thesis, University of Iowa, 1979 (unpublished).
- ¹³R. Hofstadter and H. R. Collard, in *Nuclear Radii*, edited by H. Schopper (Springer, Berlin, 1967), Group 1, Vol. 2, p. 21.
- ¹⁴L. R. Suelzle, M. R. Yearian, and H. Crannell, Phys. Rev. 162, 992 (1967).
- ¹⁵G. Hölher *et al.*, Nucl. Phys. B114, 505 (1976).
- ¹⁶G. L. Payne and B. P. Nigam, Phys. Rev. C 21, 1177 (1980).
- ¹⁷W. von Oertzen and H. G. Bohlen, Phys. Rep. 19, 1 (1975).
- ¹⁸R. E. Johnson, M. S. thesis, University of Iowa, 1980 (unpublished).